J Membrane Biol (2008) 226:27–34
DOI 10.1007/s00232-008-9136-2

Two Distinct Mechanisms of Transport Through the Plasmodial Surface Anion Channel

Abdullah A. B. Bokhari · Tsione Solomon · Sanjay A. Desai

Received: 4 August 2008 / Accepted: 15 October 2008 / Published online: 3 December 2008

Abstract The plasmodial surface anion channel (PSAC) is a voltage-dependent ion channel on erythrocytes infected with malaria parasites. To fulfill its presumed function in parasite nutrient acquisition, PSAC is permeant to a broad range of charged and uncharged solutes; it nevertheless excludes Na^+ as required to maintain erythrocyte osmotic stability in plasma. Another surprising property of PSAC is its small single-channel conductance (<3 pS in isotonic Cl^-) in spite of broad permeability to bulky solutes. While exploring the mechanisms underlying these properties, we recently identified interactions between permeating solutes and PSAC inhibitors that suggest the channel has more than one route for passage of solutes. Here, we explored this possibility with 22 structurally diverse solutes and found that each could be classified into one of two categories based on effects on inhibitor affinity, the temperature dependence of these effects and a clear pattern of behavior in permeant solute mixtures. The clear separation of these solutes into two discrete categories suggests two distinct mechanisms of transport through this channel. In contrast to most other broad-permeability channels, selectivity in PSAC appears to be complex and cannot be adequately explained by simple models that invoke sieving through rigid, noninteracting pores.

Keywords Plasmodial surface anion channel · Malaria · *Plasmodium falciparum* · Ion channel selectivity · Furosemide · Solute permeability · Erythrocyte · Antimalarial target

A. A. B. Bokhari · T. Solomon · S. A. Desai (✉)
Laboratory of Malaria and Vector Research, National Institute of Allergy and Infectious Diseases, National Institutes of Health, 12735 Twinbrook Parkway, Room 3 W-01, Rockville, MD 20852-8132, USA
e-mail: sdesai@niaid.nih.gov

Introduction

Growth and replication of the malaria parasite *Plasmodium falciparum* within human erythrocytes accounts for most of the clinical sequelae of malaria. Although this intra-erythrocytic cycle facilitates immune evasion, it hinders access to serum nutrients with low host cell membrane permeability. Presumably to overcome this barrier, the parasite increases the erythrocyte's permeability to a broad range of small solutes. Most, if not all, of these permeability changes have been attributed to the plasmodial surface anion channel (PSAC) (Desai et al. 2000), but some studies suggest a role for upregulated human ion channels (Huber et al. 2002; Egee et al. 2002; Staines et al. 2003, 2007; Verloo et al. 2004). In contrast to other proposed channels, functional polymorphisms between laboratory isolates and two separate mutants generated by in vitro selection suggest PSAC is parasite-encoded (Alkhalil et al. 2004; Hill et al. 2007; Lisk et al. 2008). Because PSAC activity is conserved in other plasmodia (Lisk and Desai 2005), this ion channel is recognized as an important antimalarial drug target.

PSAC has a number of intriguing functional properties. First, it stringently excludes the small Na^+ ion in spite of broad permeability to solutes of varying size and charge (Ginsburg et al. 1985; Desai et al. 2000; Staines et al. 2000; Lisk et al. 2008), with estimates of the Na^+ to Cl^- permeability ratio as low as 10^{-5}. This level of exclusion of a single small solute is unprecedented among other broadly permeant ion channels. It likely arose because of strong selective pressure: Na^+ exclusion is essential for parasite survival in the bloodstream because higher Na^+ permeability would lead to net NaCl uptake and osmotic lysis of infected erythrocytes. Although positively charged amines at the PSAC extracellular face provide electrostatic

repulsion and can account for part of this unusual selectivity (Cohn et al. 2003), other contributing mechanisms are likely.

Second, PSAC has a small single-channel conductance of <3 pS in isotonic Cl^-. Aside from imposing use of hypertonic recording solutions for the patch-clamp detection of single-channel currents (Alkhalil et al. 2004), a small conductance was unexpected because sieving of bulky solutes with diverse geometries suggests a wide aqueous pore. Wide pores are generally associated with high ion throughputs and, hence, large conductances. Two other broad-selectivity channels, bacterial OmpF and MscL, have conductances >1 nS in isotonic solutions, values in reasonable agreement with predictions based on known pore geometries (Rostovtseva et al. 2002; Phale et al. 2001; Cruickshank et al. 1997). (Some narrow pores also have large conductances. One key example, the BK channel, retains high selectivity for K^+ ions with a narrow selectivity filter but achieves a conductance of >250 pS by at least two mechanisms [Brelidze et al. 2003; Salkoff et al. 2006].) Because PSAC maintains a low throughput in spite of what must be a relatively wide aqueous pore, it may use yet unknown mechanisms to permit precisely controlled transport of diverse solutes.

A third unexpected property was recently identified using a transmittance-based osmotic lysis assay that quantifies PSAC-mediated organic solute uptake (Wagner et al. 2003) and has been extensively used to characterize PSAC function (Alkhalil et al. 2004; Desai et al. 2005; Kang et al. 2005; Lisk et al. 2006; Cohn et al. 2003; Hill et al. 2007). With this method, certain permeating solutes were found to adversely affect inhibitor affinity (Lisk et al. 2007). While sorbitol or alanine uptake was fully inhibited by 200 μM furosemide (consistent with a $K_{0.5}$ of 2.7 μM in single-channel studies [Alkhalil et al. 2004]), a 10-fold higher furosemide concentration was needed to achieve comparable inhibition of phenyl-trimethylammonium chloride (PhTMA-Cl) or isoleucine uptake. PhTMA-Cl and isoleucine transport were also less effectively inhibited by *NPF*-1 and phloridzin, structurally unrelated PSAC inhibitors (Kang et al. 2005; Desai et al. 2005). PhTMA-Cl and isoleucine were therefore categorized as R^+ solutes (for residual-forming), while sorbitol and alanine were grouped as R^- solutes. Importantly, these differences in inhibitor effectiveness could be abolished by reducing the temperature to 20°C or by preloading the cells with an R^- solute before measuring R^+ solute transport. Reduced inhibitor effectiveness was reproduced in tracer flux and whole-cell patch-clamp studies, indicating that it is not an artifact of the osmotic lysis assay. Because the tracer flux studies utilized a low 45 μM concentration of [^{14}C]-phenyl-trimethylammonium, an effect of high solute concentrations as required in osmotic lysis and patch-clamp experiments was also excluded.

Although there are proposals for several parasite-induced channels on the erythrocyte membrane (Staines et al. 2007), differing inhibitor efficacies for R^+ and R^- solutes cannot be easily explained by invoking transport via two or more unrelated channels because of the clear pattern of effects with multiple inhibitors and because preloading with R^- solutes abolishes the reduced efficacy against R^+ solute uptake (Lisk et al. 2007). Instead, these findings implicate uptake of R^+ and R^- solutes via a single channel that discriminates and transports the two groups of solutes differently. We hypothesized two structural models, a multioccupancy pore or two parallel routes through PSAC, that can conservatively account for the above findings. To test these and other possible models, we performed transport studies with a diverse collection of solutes. Our studies reveal that each solute can be unambiguously categorized as either R^- or R^+, strongly supporting two distinct mechanisms of transport through PSAC. They also reveal that the channel's ability to discriminate between solutes is not based on any single straightforward physicochemical property.

Materials and Methods

Parasite Culture and Osmotic Lysis Experiments

P. falciparum was cultured in O^+ human erythrocytes according to standard methods. Indo 1 and FCB laboratory isolates were evaluated and produced identical results, which were therefore pooled in analyses.

Osmotic lysis experiments were performed as described (Wagner et al. 2003). Trophozoite-infected red blood cells were enriched by percoll/sorbitol separation and washed in 150 mM NaCl and 20 mM Na_2HPO_4 (pH 7.5). To initiate PSAC-mediated uptake, cells were then resuspended at 0.25% hematocrit in buffered osmotic lysis solutions containing 20 mM Na-HEPES, 0.1 mg/mL BSA (pH 7.4) and either 280 mM uncharged permeant solute or 145 mM PhTMA-Cl. Each of these osmotic lysis solutions had a total osmolarity of ~310 mOsm. PSAC inhibitors were added from DMSO stock solutions; control experiments revealed that the DMSO carrier does not affect osmotic lysis kinetics. Osmotic swelling and lysis were then continuously followed by recording transmittance at 700 nm through the cell suspension (DU640 spectrophotometer with Peltier temperature control; Beckman Coulter, Fullerton, CA).

Experiments examining the effect of an R^- solute on the transport of R^+ solutes used 280 mM histidine (an R^- solute) added to the indicated osmotic lysis solutions. To avoid initiating solute uptake in osmotically shrunken cells, some experiments utilized preincubation of infected cells in 280 mM histidine, 150 mM NaCl, 20 mM Na_2HPO_4 (pH

7.5) for 30 min to preload histidine. This preloading did not significantly alter osmotic lysis kinetics with or without furosemide, presumably because flux through PSAC does not saturate below molar solute concentrations (Desai et al. 2000; Alkhalil et al. 2004).

Solute Structure–Activity Relationships

Solute hydrophobicity and polarity were determined as the calculated logarithm of the oil–water partition coefficient and the topological polar surface area according to algorithms in ChemDraw 10.0 (CambridgeSoft, Cambridge, MA) (Ertl et al. 2000). The molecular size of each solute was estimated as the van der Waals volume after correction for aromatic and nonaromatic rings, as described (Zhao et al. 2003).

Results

To explore the mechanistic basis of these observations, we began the present study by surveying the efficacy of known inhibitors against other solutes transported via PSAC. Figure 1a shows osmotic lysis time courses in two related solutes, proline and hydroxyproline, and reveals a surprising difference. Hydroxyproline uptake was abolished by either 200 μM furosemide or 10 μM NPPB, as indicated by negligible osmotic lysis over 90 min (blue traces in each of the upper panels, Fig. 1a). In contrast, proline-mediated lysis was slowed, but not abolished, by these inhibitors; 10-fold higher concentrations of either inhibitor were required to comparably reduce proline uptake (lower panels, Fig. 1a). Dantrolene and glybenclamide, two other known inhibitors, also required higher concentrations to inhibit

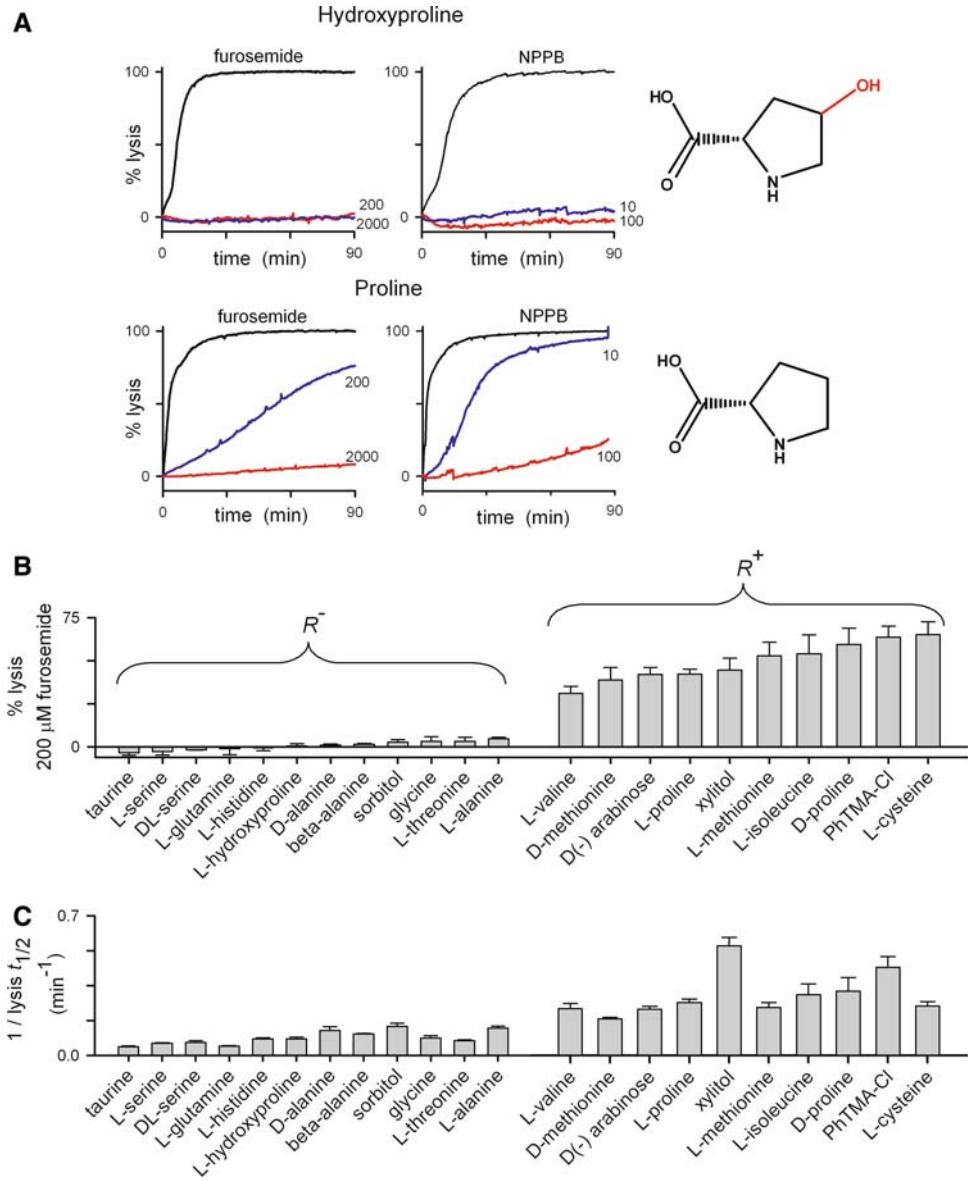

Fig. 1 Two discrete categories of permeant solutes. **a** Infected erythrocyte lysis kinetics in hydroxyproline or proline (*upper* and *lower panels*, respectively). For each solute, the *left panel* shows lysis kinetics with 0, 200 and 2,000 μM furosemide (black, blue and red traces, respectively); the *right panel* shows separate experiments with 0, 10 and 100 μM NPPB. The structures of these two solutes are also shown, with the difference highlighted in red. **b** Residual uptake for 22 solutes, quantified as the percentage osmotic lysis after 60 min in the solute with 200 μM furosemide. Each bar represents the mean ± SEM from up to 15 continuous transmittance recordings relative to matched recordings without furosemide. Solutes are ordered according to increasing residual uptake to emphasize the difference between the two groups. **c** Relative solute permeability coefficients, determined as the reciprocal of the time to 50% lysis without inhibitors

proline transport than to inhibit hydroxyproline transport (not shown).

We examined lysis kinetics in 22 solutes using this approach. The selected solutes met several important criteria in control experiments not shown here. Each had relatively high infected cell permeability, corresponding to completion of osmotic lysis within 60 min. We also excluded solutes producing measurable osmotic lysis of uninfected cells to avoid contributions from unmodified endogenous transporters. Finally, uptake of each selected solute was abolished by saturating concentrations of *NPF*-1, a specific inhibitor that confirms uptake primarily via PSAC (Kang et al. 2005).

To explore the effects of solute substructure and stereochemistry, we included a number of nonphysiological amino acids. Figure 1b tallies these solutes and their residual transport magnitudes. These studies revealed two distinct categories: 12 solutes produced negligible osmotic lysis with 200 μM furosemide and are therefore R^- solutes, following our previous nomenclature (Lisk et al. 2007); the remaining 10 solutes exhibited significant residual lysis and are classified as R^+ solutes. For all 22 solutes, 2 mM furosemide abolished osmotic lysis over a 60-min period (red traces in Fig. 1a, not shown for other solutes), consistent with transport via one of two discrete PSAC-associated mechanisms.

Figure 1c shows the relative permeability coefficients for each of these solutes, calculated as the reciprocal of the inhibitor-free lysis half-time (Wagner et al. 2003). Although R^+ solutes as a group had somewhat higher permeabilities than R^- solutes, this difference is not sufficient to account for the dramatic difference in inhibitor effectiveness between the two groups.

To quantify the effect of solute permeabilities on furosemide efficacy, we performed additional experiments and devised the parameter described in Fig. 2a. For each R^-

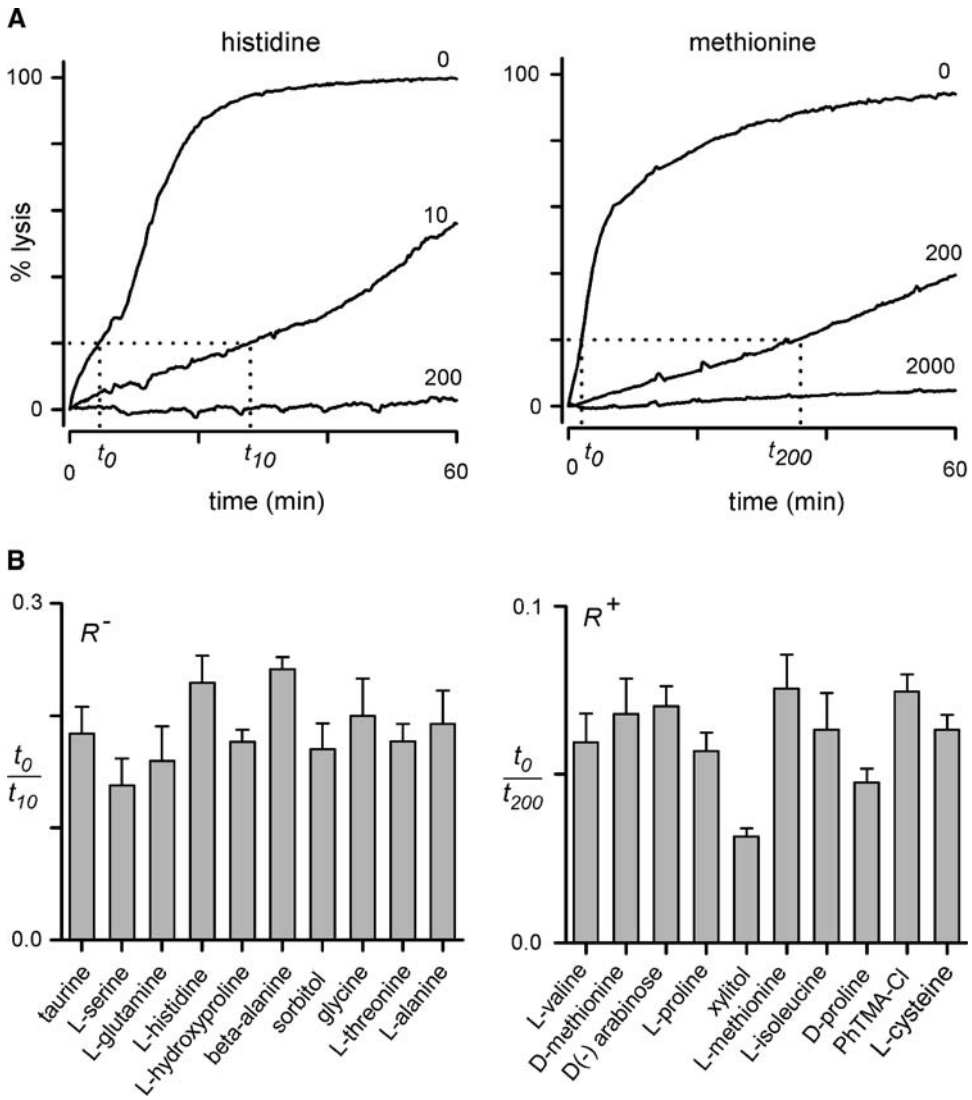

Fig. 2 Furosemide affinities for R^- solutes do not differ significantly, but those of some R^+ solutes do. **a** Osmotic lysis kinetics for L-histidine and L-methionine (representative R^- and R^+ solutes, respectively) with micromolar furosemide concentrations indicated to the *right* of each trace. *Superimposed dotted lines* represent the approach used to determine the time to 20% lysis without or with furosemide (t_0 and t_{10} or t_{200}, respectively). **b** Mean ± SEM of the ratios t_0/t_{10} for R^- solutes and t_0/t_{200} for R^+ solutes (determined from up to 15 trials for each solute). Furosemide's inhibitory affinity is inversely proportional to these ratios. Because they were measured using different furosemide concentrations, it is not appropriate to compare the values in one panel with those in the other

solute, we tracked lysis kinetics without and with 10 μM furosemide, a concentration that produces slowed but measurable uptake on reasonable time scales; similar experiments were performed with R^+ solutes except that a higher furosemide concentration (200 μM) was required to produce comparable inhibition (Fig. 2a). Because there is an inverse relationship between the time to a given level of lysis and the solute's permeability, the ratio of time to a threshold level of lysis without and with furosemide (t_0/t_{10} or t_0/t_{200}) provides a quantitative estimate of furosemide efficacy independent of each solute's intrinsic permeability. The two panels in Fig. 2b show the mean value for this ratio for each solute. Although there was some variation between solutes within each group, most of these differences were not statistically significant, suggesting identical furosemide affinities within each category. However, we did find that the t_0/t_{200} ratios for PhTMA-Cl and xylitol were statistically significant ($P < 10^{-4}$, $n = 6$–8 each, unpaired two-tailed Student's t-test). The possible mechanisms behind this difference are currently under study.

We previously found that a modest reduction in temperature abolishes residual PhTMA-Cl uptake with 200 μM furosemide (Lisk et al. 2007). We therefore examined whether this is a general feature for all R^+ solutes by following osmotic lysis kinetics with each R^+ solute at 37°C and 15°C (Fig. 3). Lowering the temperature had only a modest effect when furosemide was absent (green versus black trace in each panel), consistent with the weak temperature dependence of aqueous phase diffusion through pores. In contrast, the same temperature decrease produced a marked effect when 200 μM furosemide was present: the residual lysis characteristic of R^+ solutes was no longer detectable for any solute (blue versus red traces). This steep temperature dependence for furosemide affinity was not seen in transport studies with R^- solutes (Lisk et al. 2007), indicating that it is specific to R^+ solute transport and further supporting the classification of solutes into two groups.

In the previous study, residual PhTMA-Cl or isoleucine transport was similarly abolished by measurement in the presence of either sorbitol or alanine. Competition between solutes for a shared route could not explain these observations because PhTMA-Cl and isoleucine did not similarly affect each other's transport. Instead, it suggested a controlling effect of R^- solutes over the low furosemide affinity mechanism available only to R^+ solutes. We therefore tested whether this controlling effect is also present with the newly identified R^+ and R^- solutes. Figure 4a shows that proline transport with 200 μM furosemide is abolished by addition of the R^- solute histidine, while its transport without furosemide is only modestly affected. Each of the other R^- solutes also had this controlling effect on residual proline transport (not shown). Histidine also abolished the residual transport of every R^+ solute (Fig. 4b). These findings are consistent with a modulatory role of R^- solutes on the residual transport of R^+ solutes; they support our model of a shared low furosemide affinity mechanism for all R^+ solutes. These findings are inconsistent with models invoking residual transport via mechanisms unrelated to PSAC because physically separate channels cannot achieve interactions between the two solute groups.

How does PSAC distinguish between R^+ and R^- solutes? Presumably, R^+ solutes share one or more physicochemical properties that permit their collective recognition by a selectivity filter in the channel. Quantitative measures of molecular size, hydrophobicity and polarity did not reveal unambiguous correlations with residual osmotic lysis magnitudes (Fig. 5), suggesting a multifaceted basis for recognition of R^- versus R^+ solutes.

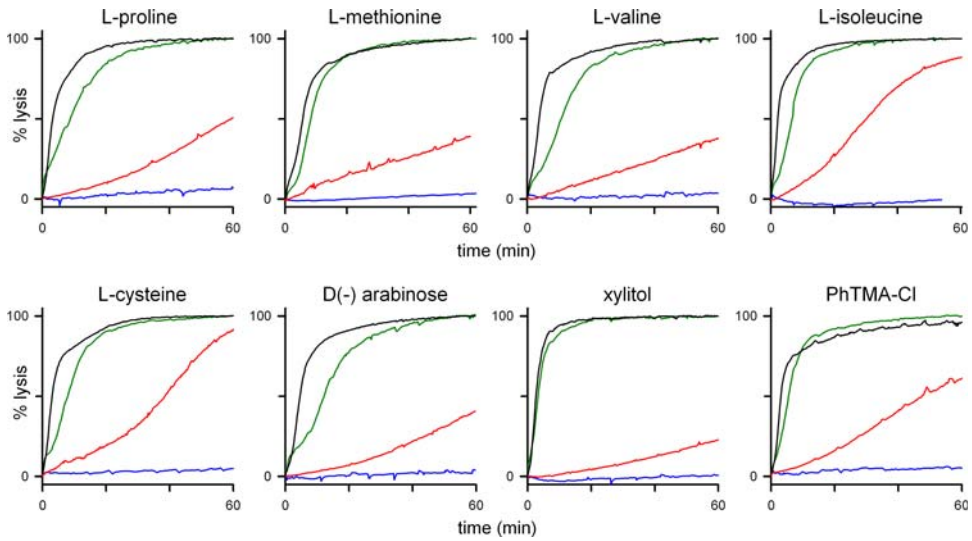

Fig. 3 Steep temperature dependence of residual transport. Each panel shows osmotic lysis kinetics for the indicated R^+ solute at 37°C (black and red traces) and 15°C (green and blue traces) without (black and green) or with (red and blue) 200 μM furosemide. Traces are typical of $n = 3$ for each solute. Reducing the temperature had only a modest effect without inhibitor but abolished PSAC-mediated lysis when furosemide was present. D-Methionine and D-proline also exhibited this effect with kinetics similar to their L-isomers (not shown)

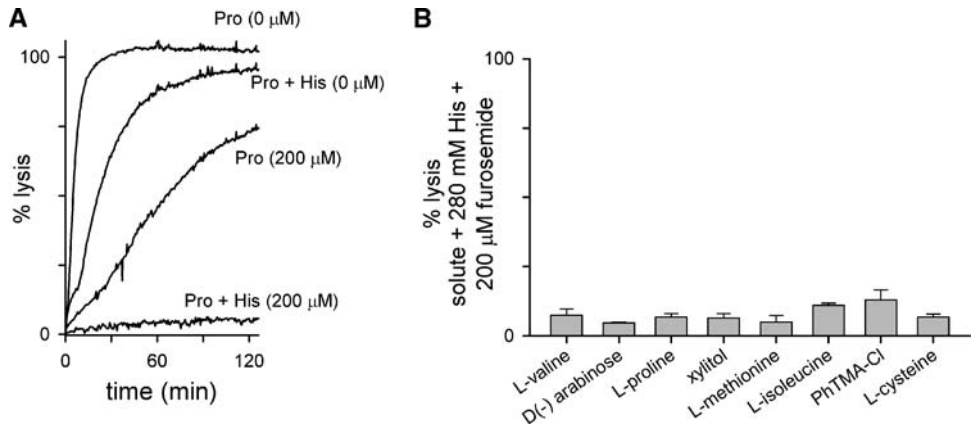

Fig. 4 Addition of an R^- solute abolishes residual transport of R^+ solutes. **a** Osmotic lysis kinetics at 37°C in L-proline in the presence or absence of 280 mM histidine, as indicated by standard three-letter amino acid abbreviations. Furosemide concentrations for each recording are indicated in parentheses. Histidine has a modest competitive effect on proline uptake without inhibitors, but it largely abolishes proline uptake when 200 μM furosemide is present. **b** Residual uptake for each R^+ solute measured in the presence of 280 mM histidine. Each bar represents the mean ± SEM percentage lysis after 60 min in the solute mixture with 200 μM furosemide relative to a matched recording without furosemide ($n = 3$–8 trials each). These experiments are identical to those in Fig. 1c except for the addition of histidine to each solute. Addition of histidine abolishes the residual uptake of each R^+ solute

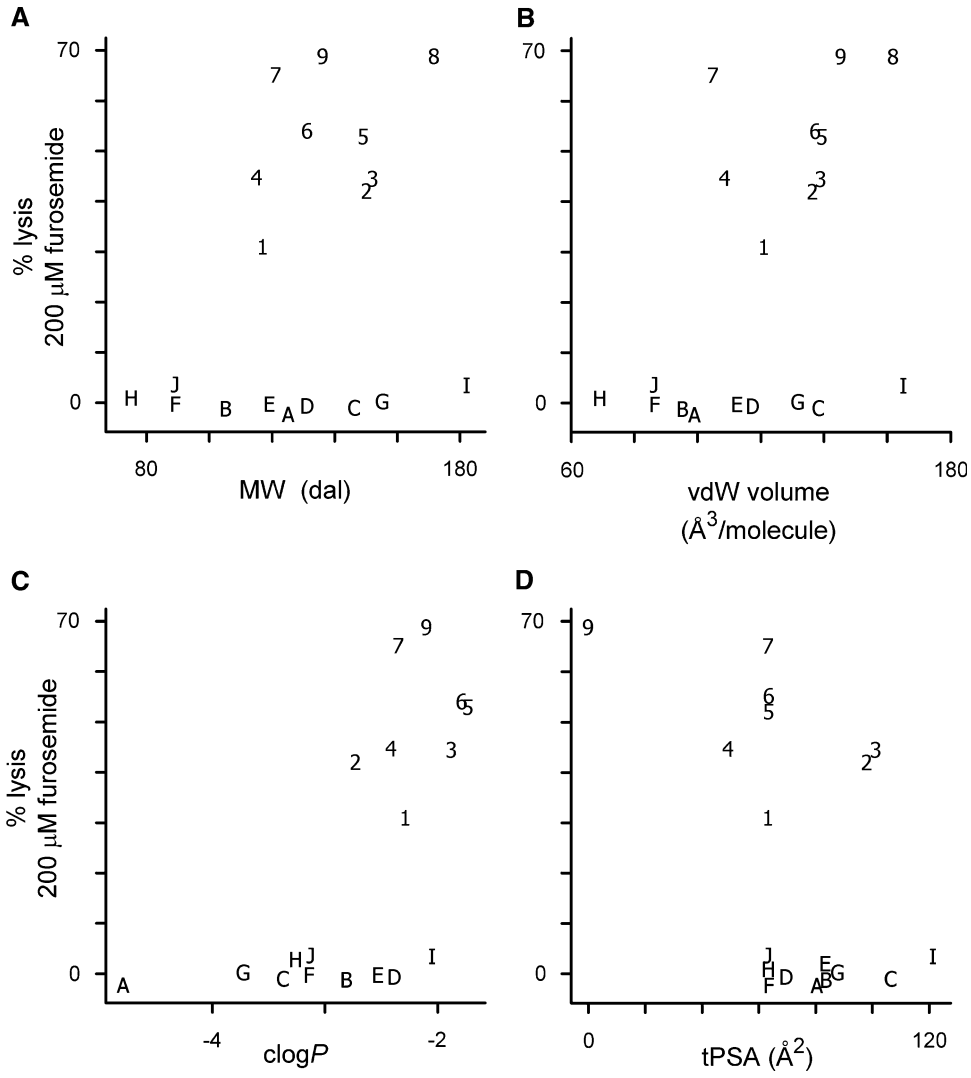

Fig. 5 Individual physicochemical properties of permeant solutes do not predict access to the two mechanisms. Mean percentage osmotic lysis values with furosemide from Fig. 1b (37°C, 60 min) are plotted against solute molecular weight, van der Waals volume, calculated logarithm of the oil–water partition coefficient (clog*P*) and topological polar surface area (tPSA) (**a**–**d**, respectively), as described in "Materials and Methods." R^- and R^+ solutes are represented by letters and numbers as follows: A, taurine; B, serine; C, glutamine; D, hydroxyproline; E, threonine; F, *β*-alanine; G, histidine; H, glycine; I, sorbitol; J, alanine; 1, valine; 2, arabinose; 3, xylitol; 4, proline; 5, methionine; 6, isoleucine; 7, cysteine; 8, PhTMA-Cl salt; 9, $PhTMA^+$ cation. Enantiomeric amino acids in Fig. 1b have identical values for each physicochemical parameter. The parameters in **c** and **d** could not be calculated for PhTMA-Cl salt

Discussion

The present study extends the original observation of solute–inhibitor interactions (Lisk et al. 2007) by demonstrating similar effects for a larger collection of permeating solutes. Approximately half of the 22 solutes examined here exhibited significant residual transport with 200 μM furosemide, leading to their classification as R^+ solutes. For each of these solutes, the reduction in inhibitor efficacy was quantitatively similar as a 10-fold increase in furosemide concentration invariably abolished osmotic lysis. This pattern is also conserved with other inhibitors, for which R^+ solutes also reduce efficacy by approximately 10-fold (Lisk et al. 2007, and unpublished observations); why these reductions are quantitatively similar is currently under study. Also conserved for these new R^+ solutes is the steep temperature dependence of transport remaining with 200 μM furosemide: reducing the temperature to 20°C or lower abolishes residual transport and eliminates the differences between R^+ and R^- solutes. The residual transport of each R^+ solute can also be abolished by preloading cells with an R^- solute. This collection of observations strongly implicates transport of each of these solutes by one of two distinct mechanisms in a single ion channel.

One explanation that can account for our findings is that there are two separate routes for transport through PSAC; these routes are distinguished by differing affinities for furosemide and other available inhibitors. In this scenario, R^+ solutes would have access to both routes while R^- solutes would be transported only by the more furosemide-sensitive route. The differing temperature dependence for R^+ solute transport with and without furosemide is particularly suggestive of physically separate routes. Another explanation is a single multioccupancy pore where binding of an R^+ solute interferes with inhibitor access in a temperature-dependent manner; in this case, simultaneous occupancy of the pore by an R^- solute would overcome this interference and restore inhibitor efficacy. While there is precedence for both of the above explanations in other ion channels, it is also possible that the observed transport complexities reflect early evidence for a yet unknown mechanism of solute recognition and handling.

Our analysis of these two groups of solutes provides several new insights. First, R^+ solutes have modest, but consistently higher permeabilities than R^- solutes, as quantified by osmotic lysis halftimes (Fig. 1c). Although there are alternative explanations for this trend, this greater permeability may reflect the proposed access of R^+ solutes to an additional route through the channel. This trend, however, is not sufficient to account for the distinctly different furosemide efficacies for the two groups of solutes.

A dramatic example of PSAC's ability to discriminate between these groups is the observation that a single hydroxyl substitution on the pyrrolidine ring of proline converts it from an R^+ solute into an R^- solute; other examples are also apparent in Fig. 1b. Such fine-tuning of selectivity is commonplace for carrier-type mechanisms but has less precedence in ion channels with broad permeability profiles. The responsible selectivity filter does not appear to distinguish between stereoisomers as our studies with four enantiomeric pairs of amino acids did not reveal significant differences in furosemide efficacy.

We explored solute structure–activity relationships that may explain how permeant solutes are classified into two groups. Quantitative parameters of solute size, hydrophobicity and polarity did not reveal a clear correlation with the residual phenotype, suggesting that complex interactions with unidentified channel components determine whether a permeating solute behaves as an R^- or an R^+. A more definitive understanding of the two discrete mechanisms of transport described here may require identification of PSAC's gene(s), development of a heterologous expression system that reproduces these solute–inhibitor interactions and functional studies of engineered site-directed channel mutants. In any case, a rigid selectivity filter that only passively interacts with solutes does not adequately explain permeation through PSAC.

Finally, regardless of the structural basis of these solute–inhibitor interactions, these findings have significant implications for drug discovery and development targeting PSAC. In vitro parasite growth inhibition by antagonists is consistent with PSAC's proposed physiological role in parasite nutrient uptake (Desai et al. 2000). Because our studies suggest that about half of these nutrients will behave as R^+ solutes, complete inhibition of both nutrient uptake and parasite growth may require higher inhibitor concentrations than expected from previous patch-clamp studies. One hopes it is possible to identify inhibitors not susceptible to these affinity-reducing interactions with R^+ solutes; such compounds may be better starting points for antimalarial drug development targeting PSAC.

Acknowledgements We thank Wang Nguitragool and Ajay Pillai for helpful comments. This research was supported by the Intramural Research Program of the National Institutes of Health, National Institute of Allergy and Infectious Diseases and by the Medicines for Malaria Venture.

References

Alkhalil A, Cohn JV, Wagner MA, Cabrera JS, Rajapandi T, Desai SA (2004) *Plasmodium falciparum* likely encodes the principal anion channel on infected human erythrocytes. Blood 104:4279–4286

Brelidze TI, Niu X, Magleby KL (2003) A ring of eight conserved negatively charged amino acids doubles the conductance of BK channels and prevents inward rectification. Proc Natl Acad Sci USA 100:9017–9022

Cohn JV, Alkhalil A, Wagner MA, Rajapandi T, Desai SA (2003) Extracellular lysines on the plasmodial surface anion channel involved in Na^+ exclusion. Mol Biochem Parasitol 132:27–34

Cruickshank CC, Minchin RF, Le Dain AC, Martinac B (1997) Estimation of the pore size of the large-conductance mechanosensitive ion channel of *Escherichia coli*. Biophys J 73:1925–1931

Desai SA, Bezrukov SM, Zimmerberg J (2000) A voltage-dependent channel involved in nutrient uptake by red blood cells infected with the malaria parasite. Nature 406:1001–1005

Desai SA, Alkhalil A, Kang M, Ashfaq U, Nguyen ML (2005) Plasmodial surface anion channel–independent phloridzin resistance in *Plasmodium falciparum*. J Biol Chem 280:16861–16867

Egee S, Lapaix F, Decherf G, Staines HM, Ellory JC, Doerig C, Thomas SL (2002) A stretch-activated anion channel is upregulated by the malaria parasite *Plasmodium falciparum*. J Physiol 542:795–801

Ertl P, Rohde B, Selzer P (2000) Fast calculation of molecular polar surface area as a sum of fragment-based contributions and its application to the prediction of drug transport properties. J Med Chem 43:3714–3717

Ginsburg H, Kutner S, Krugliak M, Cabantchik ZI (1985) Characterization of permeation pathways appearing in the host membrane of *Plasmodium falciparum* infected red blood cells. Mol Biochem Parasitol 14:313–322

Hill DA, Pillai AD, Nawaz F, Hayton K, Doan L, Lisk G, Desai SA (2007) A blasticidin S–resistant *Plasmodium falciparum* mutant with a defective plasmodial surface anion channel. Proc Natl Acad Sci USA 104:1063–1068

Huber SM, Uhlemann AC, Gamper NL, Duranton C, Kremsner PG, Lang F (2002) *Plasmodium falciparum* activates endogenous Cl^- channels of human erythrocytes by membrane oxidation. EMBO J 21:22–30

Kang M, Lisk G, Hollingworth S, Baylor SM, Desai SA (2005) Malaria parasites are rapidly killed by dantrolene derivatives specific for the plasmodial surface anion channel. Mol Pharmacol 68:34–40

Lisk G, Desai SA (2005) The plasmodial surface anion channel is functionally conserved in divergent malaria parasites. Eukaryot Cell 4:2153–2159

Lisk G, Kang M, Cohn JV, Desai SA (2006) Specific inhibition of the plasmodial surface anion channel by dantrolene. Eukaryot Cell 5:1882–1893

Lisk G, Scott S, Solomon T, Pillai AD, Desai SA (2007) Solute–inhibitor interactions in the plasmodial surface anion channel reveal complexities in the transport process. Mol Pharmacol 71:1241–1250

Lisk G, Pain M, Gluzman IY, Kambhampati S, Furuya T, Su XZ, Fay MP, Goldberg DE, Desai SA (2008) Changes in the plasmodial surface anion channel reduce leupeptin uptake and can confer drug resistance in *P. falciparum*–infected erythrocytes. Antimicrob Agents Chemother 52:2346–2354

Phale PS, Philippsen A, Widmer C, Phale VP, Rosenbusch JP, Schirmer T (2001) Role of charged residues at the OmpF porin channel constriction probed by mutagenesis and simulation. Biochemistry 40:6319–6325

Rostovtseva TK, Nestorovich EM, Bezrukov SM (2002) Partitioning of differently sized poly(ethylene glycol)s into OmpF porin. Biophys J 82:160–169

Salkoff L, Butler A, Ferreira G, Santi C, Wei A (2006) High-conductance potassium channels of the SLO family. Nat Rev Neurosci 7:921–931

Staines HM, Rae C, Kirk K (2000) Increased permeability of the malaria-infected erythrocyte to organic cations. Biochim Biophys Acta 1463:88–98

Staines HM, Powell T, Ellory JC, Egee S, Lapaix F, Decherf G, Thomas SL, Duranton C, Lang F, Huber SM (2003) Modulation of whole-cell currents in *Plasmodium falciparum*–infected human red blood cells by holding potential and serum. J Physiol 552:177–183

Staines HM, Alkhalil A, Allen RJ, De Jonge HR, Derbyshire E, Egee S, Ginsburg H, Hill DA, Huber SM, Kirk K, Lang F, Lisk G, Oteng E, Pillai AD, Rayavara K, Rouhani S, Saliba KJ, Shen C, Solomon T, Thomas SL, Verloo P, Desai SA (2007) Electrophysiological studies of malaria parasite–infected erythrocytes: current status. Int J Parasitol 37:475–482

Verloo P, Kocken CH, van der WA, Tilly BC, Hogema BM, Sinaasappel M, Thomas AW, De Jonge HR (2004) *Plasmodium falciparum*–activated chloride channels are defective in erythrocytes from cystic fibrosis patients. J Biol Chem 279:10316–10322

Wagner MA, Andemariam B, Desai SA (2003) A two-compartment model of osmotic lysis in *Plasmodium falciparum*–infected erythrocytes. Biophys J 84:116–123

Zhao YH, Abraham MH, Zissimos AM (2003) Fast calculation of van der Waals volume as a sum of atomic and bond contributions and its application to drug compounds. J Org Chem 68:7368–7373